Journal of Natural Gas Science and Engineering 24 (2015) 279–290

Contents lists available at ScienceDirect

Journal of Natural Gas Science and Engineering

journal homepage: www.elsevier.com/locate/jngse

Production forecasting of gas condensate well considering fluid phase behavior in the reservoir and wellbore

Juntai Shi [a, *], Liang Huang [a], Xiangfang Li [a], Kamy Sepehrnoori [b]

[a] MOE Key Laboratory of Petroleum Engineering, China University of Petroleum at Beijing, Beijing 102249, PR China
[b] The University of Texas at Austin, Austin, TX 78712, USA

ARTICLE INFO

Article history:
Received 19 November 2014
Received in revised form
20 March 2015
Accepted 22 March 2015
Available online

Keywords:
Gas condensate wells
Deliverability equations
Fluid phase behavior
Wellbore
Pseudo-pressure function
Two phase flow

ABSTRACT

Retrograde condensation occurs when the reservoir pressure falls below the dew point pressure in gas condensate reservoirs. Complex fluid phase behavior in the reservoir and the wellbore makes it challenging to predict the productivity of gas condensate wells. To date, the gas rate in the deliverability equation of gas well is assumed the gas rate at surface condition converted from that at the reservoir condition by using the volume factor. However, because of the complex fluid phase behavior in gas condensate wells, the gas rate at the reservoir condition cannot be directly changed to that at surface condition by using volume factor. Hence, the development of a new analytical model to accurately calculate the productivity of gas condensate wells is still required and necessary.

In this work, we propose a new deliverability equation of gas condensate wells with a consideration of fluid phase behavior in both the reservoir and the wellbore. Also, several pseudo-pressure functions for different condensate distribution and flow models are examined systematically; these include the model before condensation, the model after condensation, but without condensate flow, the model after condensation and with condensate flow, and the model after re-vaporization. Two synthetic numerical simulation cases and two field case studies are performed to validate these deliverability equations for gas condensate wells.

Results show that the phase behavior of gas condensate fluid in the wellbore plays a significant role in the deliverability evaluation and in the forecasting of gas condensate wells. If neglecting its effect on the deliverability, gas and condensate production rates could not be accurately predicted. The data from the proposed model have good agreement with the simulation and field production data of wells in Yakela Gas Condensate Reservoir and Yaha Gas Condensate Reservoir in China. If the conventional deliverability equation neglecting the effect of phase behavior in the wellbore was used, the predicted gas production will be higher than the actual value; even 50% higher than the actual value at high flow rates. Through these case studies, it can be concluded that the effect of condensate-gas phase behavior in the wellbore cannot be ignored in the deliverability equation for gas condensate wells.

This work can provide a more accurate method of forecasting the gas and condensate production for condensate gas reservoirs and also guide optimization of single well production rate and gas recovery rate for gas condensate reservoirs.

1. Introduction

Gas condensate reservoir is a special complex reservoir. In the production process, the condensate liquid will retrograde, gradually accumulate, and then form condensate blocking in the vicinity of wellbore after the bottom-hole flowing pressure (BHFP) has dropped below the dew point pressure (Muskat and Meres, 1936; Fevang and Whitson, 1995; Whitson et al., 1999; Henderson et al., 2000). The condensate blocking would decrease the productivity of gas condensate well. Many researchers have proposed different types of deliverability equations for gas condensate wells, which can be summarized into four types: the deliverability equation for conventional gas wells (Houpeurt, 1959; Rawlins and Schellhardt, 1935) in which the gas flow rate is assumed the sum of pure gas flow rate and condensate converted gas flow rate (Li, 2008; Shi

* Corresponding author.
E-mail address: juntai.shi@gmail.com (J. Shi).

http://dx.doi.org/10.1016/j.jngse.2015.03.033
1875-5100/

et al., 2010, 2013); the deliverability equation in which the condensate blocking effect is considered as another skin factor (Fetkovich, 1973; Kniazeff and Naville, 1965; Gondouin and Husson, 1967a,b); the deliverability equation with steady pseudo-pressure function (O'Dell and Miller, 1967; Fussell, 1972; Jones and Raghavan, 1985; He et al., 1996); the deliverability equation with pseudo-pressure function at pseudo-steady condition (Fevang and Whitson, 1995; Xie et al., 2001). For gas condensate reservoirs, phase behavior changes not only in the formation but also in the wellbore during the whole production life. At present, the phase behavior in the wellbore was ignored in most of deliverability equations, and the volume factor was used to represent the relationship between flow rate in the bottom-hole and in the wellhead. For the gas condensate well, the composition of gas phase and condensate phase at the bottom-hole is not the same as that at surface. Thus, the volume factor of gas and condensate should not be used in the formulation of deliverability equation of gas condensate wells. In this work, we propose a new deliverability equation of gas condensate well considering fluid phase behavior in both the reservoir and the wellbore. And several pseudo-pressure functions for different condensate saturation distributions and flow models are considered, including model before condensation, model after condensation but without condensate flow, model after condensation with condensate flow, and model after re-vaporization. The relationship between flow rate in the bottom-hole and in the wellhead is obtained based on the phase behavior. Case studies are conducted to validate the effectiveness of these deliverability equations proposed in this work.

2. Phase behavior and condensate distribution in gas condensate reservoir

2.1. Phase envelop for gas condensate system

Fig. 1 shows the phase envelope of a gas condensate system in which the reservoir temperature is between the critical temperature and the cricondentherm, and reservoir pressure is larger than the dew point pressure. During the production, the temperature remains constant. As the reservoir pressure declines, shown as vertical line AH in Fig. 1, it goes through the upper dew point B from point A at the reservoir temperature and liquid begins to precipitate out of the gas phase. Then the pressure sequentially goes through the upper mobile condensate point D and the maximum liquid saturation point E, after which liquid partly re-vaporizes to become gas phase again, and the lower mobile condensate is obtained at point F. In some cases, the vertical line goes through the lower dew point G to reach point H and liquid totally re-vaporizes to become gas phase. Pressures for points A, B, D, E, F, and G respectively denote the initial reservoir pressure p_e, the upper dew point pressure $p_{d,up}$, the upper mobile condensate point pressure p^*_{up}, the maximum liquid saturation point pressure $p_{max,So}$, the lower mobile condensate point pressure p^*_{down} and the lower dew point pressure $p_{d,down}$.

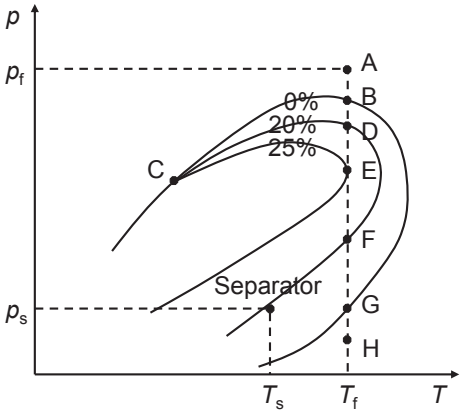

Fig. 1. *PT* phase diagram for a gas condensate system.

2.2. Condensate distribution and flow models in gas condensate reservoirs

The condensate distribution near the wellbore and/or in the formation will change as the BHFP drops at a given flow rate. However, under the steady state which is reasonable for short-term production, the reservoir pressure and the BHFP remain constant at a given flow rate and the condensate distribution near the wellbore and/or in the formation will not change. At different production stages, according to BHFP, the corresponding condensate distribution and flow models are investigated as follows.

(1) Two-zone model

Condensate distribution model without condensate flow is actually two-zone condensate distribution model, as shown in the figures in the Shi et al. (2010) paper. In the outer region of gas condensate reservoir where the pressure is higher than the upper dew point pressure, only single gas phase exists and flows, while in the inner region of gas condensate reservoir where the pressure is lower than the upper dew point pressure but higher than the upper mobile condensate point pressure, condensate appears but does not flows. On account of the condensate blockage (Muskat and Meres, 1936), or the "condensate blocking" (Fevang, 1995; Whitson, 1999; Henderson, 2000), in the inner region of gas condensate reservoir, the deliverability of gas condensate reservoirs decreases.

(2) Three-zone model

When the condensate saturation near the wellbore becomes larger than the critical flow saturation (with decreasing BHFP), three zones of condensate distribution and flow pattern will appear as shown figures in the reference (Shi et al., 2010). The three-zone model (Fevang and Whiston, 1995; Ali et al., 1997) should be applied; here both gas and condensate oil flow simultaneously but at different velocities in an inner near-wellbore region, which is called the "two-phase flow regime". In this zone gas-oil ratio (GOR) is equal to the producing GOR of the gas well (Du et al., 2004).

(3) Four-zone model

After BHFP drops below the maximum liquid saturation point pressure, condensate saturation decreases again, and when it becomes less than the critical flow saturation, condensate in this zone will become immobile again, which is called the 4th zone; hence the four-zone model will appear, as shown in figures in the reference (Shi et al., 2010).

3. Pseudo-pressure function for gas condensate reservoir

3.1. Pseudo-pressure function for single gas phase

Before retrograde condensate occurs, single gas phase exists in both the vicinity of wellbore and the formation. The pseudo-pressure function can be expressed as

$$\psi_1 = k_{rg}(S_{wi}) \int_{p_0}^{p} \left(\frac{\rho_g}{\mu_g}\right) dp \tag{1}$$

where p is in the range of $p_{d,up} < p_{wf} < p < p_e$.

The pseudo-pressure difference between the formation and the wellbore, which appears in the deliverability equation, will be given by

$$\psi_e - \psi_{wf} = k_{rg}(S_{wi}) \int_{p_{wf}}^{p_e} \left(\frac{\rho_g}{\mu_g}\right) dp \tag{2}$$

3.2. Pseudo-pressure function for two-zone model

When retrograde condensation occurs but only gas flows, and the steady state is achieved, the two-zone condensate distribution pattern will appear. Pseudo-pressure function for each zone can be displayed as follows.

Pseudo-pressure function for Zone 1 where only gas phase coexists is shown as Eq. (1), where p is between $p_{d,up}$ and p_e.

Pseudo-pressure function for Zone 2 where gas and condensate coexist but only gas flows is

$$\psi_2 = \int_{p_0}^{p} \left(\rho_g \frac{k_{rg}}{\mu_g}\right) dp, \tag{3}$$

where p is in the range of $p^*_{up} < p_{wf} < p < p_{d,up}$.

The total pseudo-pressure difference between the formation and the wellbore which appears in the deliverability equation will be the sum of the pseudo-pressure difference of these two zones, as shown in Eq. (4).

$$\begin{aligned}\psi_e - \psi_{wf} &= \left(\psi_e - \psi_{d,up}\right)_1 + \left(\psi_{d,up} - \psi_{wf}\right)_2 \\ &= k_{rg}(S_{wi}) \int_{p_{d,up}}^{p_e} \left(\frac{\rho_g}{\mu_g}\right) dp + \int_{p_{wf}}^{p_{d,up}} \left(\rho_g \frac{k_{rg}}{\mu_g}\right) dp\end{aligned} \tag{4}$$

3.3. Pseudo-pressure function for three zone model

When condensate moves and the steady state is obtained, the three-zone condensate distribution model will apply. Pseudo-pressure function for each zone can be displayed as follows:

Pseudo-pressure function for Zone 1 where only gas phase exists is represented by Eq. (1), where p is between $p_{d,up}$ and p_e. Pseudo-pressure function for Zone 2 where gas and condensate coexist but only gas flows is represented by Eq. (3), where p is between p^*_{up} and $p_{d,up}$.

Pseudo-pressure function for Zone 3 where both gas and condensate flow is

$$\psi_3 = \int_{p_0}^{p} \left(\rho_o \frac{k_{ro}}{\mu_o} + \rho_g \frac{k_{rg}}{\mu_g}\right) dp \tag{5}$$

where p is in the range of $p^*_{down} < p_{wf} < p < p^*_{up}$.

The total pseudo-pressure difference between the formation and the wellbore is the sum of pseudo-pressure difference of these three zones, as shown in Eq. (6).

$$\begin{aligned}\psi_e - \psi_{wf} &= \left(\psi_e - \psi_{d,up}\right)_1 + \left(\psi_{d,up} - \psi^*_{up}\right)_2 + \left(\psi^*_{up} - \psi_{wf}\right)_3 \\ &= k_{rg}(S_{wi}) \int_{p_{d,up}}^{p_e} \left(\frac{\rho_g}{\mu_g}\right) dp + \int_{p^*_{up}}^{p_{d,up}} \left(\rho_g \frac{k_{rg}}{\mu_g}\right) dp \\ &\quad + \int_{p_{wf}}^{p^*_{up}} \left(\rho_o \frac{k_{ro}}{\mu_o} + \rho_g \frac{k_{rg}}{\mu_g}\right) dp\end{aligned} \tag{6}$$

3.4. Pseudo-pressure function for four-zone model

When condensate changes from mobile to immobile again, and steady state is reached, the four-zone condensate distribution model will appear. Pseudo-pressure function for each zone can be displayed as follows.

Pseudo-pressure function for Zone 1 and 2 are the same as those in three zone model. Pseudo-pressure function for Zone 3 is represented by Eq (5), where p is between p^*_{down} and p^*_{up}.

Pseudo-pressure function for Zone 4 where condensate oil is immobile again is

$$\psi_4 = \int_{p_0}^{p} \left(\rho_g \frac{k_{rg}}{\mu_g}\right) dp \tag{7}$$

where p is between p_{wf} and p^*_{down}.

The total pseudo-pressure difference in the steady-state deliverability equation of gas condensate well is the sum of the four regions' pseudo-pressure difference, which is

$$\begin{aligned}\psi_e - \psi_{wf} &= \left(\psi_e - \psi_{d,up}\right)_1 + \left(\psi_{d,up} - \psi^*_{up}\right)_2 + \left(\psi^*_{up} - \psi^*_{down}\right)_3 + \left(\psi^*_{down} - \psi_{wf}\right)_4 \\ &= k_{rg}(S_{wi}) \int_{p_{d,up}}^{p_e} \left(\frac{\rho_g}{\mu_g}\right) dp + \int_{p^*_{up}}^{p_{d,up}} \left(\rho_g \frac{k_{rg}}{\mu_g}\right) dp + \int_{p^*_{down}}^{p^*_{up}} \left(\rho_o \frac{k_{ro}}{\mu_o} + \rho_g \frac{k_{rg}}{\mu_g}\right) dp + \int_{p_{wf}}^{p^*_{down}} \left(\rho_g \frac{k_{rg}}{\mu_g}\right) dp\end{aligned} \tag{8}$$

4. Relationship of flow rate between bottom-hole and wellhead

In order to get more reasonable gas condensate reservoir deliverability equations which reflect the complex fluid-phase-change characteristics in the wellbore, it is important to get the relationship of gas flow rate between bottom-hole and well-head.

4.1. Relationship of flow rate between bottom-hole and well-head before retrograde condensation

For a gas condensate reservoir with formation pressure higher than dew point pressure, in the case of low gas proration of gas condensate well or in the early stage of production, the BHFP is higher than the dew point pressure of original fluid after achieving stability. Single-phase gas flows in the reservoir, but condensate and gas flow may occur in the wellbore. The relationship of production between bottom-hole and wellhead is shown below.

The condensate oil volume fraction of the mixture under the wellhead condition is obtained using fluid mixture from the wellhead, which is expressed as

$$V_{\mathrm{roCCE}}(p_{\mathrm{sc}}) = \frac{V_{\mathrm{o}}}{V_{\mathrm{g}} + V_{\mathrm{o}}} = \frac{q_{\mathrm{o,sc}}}{q_{\mathrm{g,sc}} + q_{\mathrm{o,sc}}} \tag{9}$$

Subsequently, the wellhead condensate oil production can be obtained, which is

$$q_{\mathrm{o,sc}} = \frac{q_{\mathrm{g,sc}} V_{\mathrm{roCCE}}(p_{\mathrm{sc}})}{1 - V_{\mathrm{roCCE}}(p_{\mathrm{sc}})} \tag{10}$$

Because the gas condensate well produces steadily, according to the constant composition expansion experiment (CCE), the underground condensate gas composition is the same as that at the surface. As the BHFP is greater than the dew point pressure of fluid mixture, there is only condensate gas and no condensate oil in the bottom-hole.

Based on mass conservation, the mass of the bottom-hole condensate gas is equal to the total mass of wellhead natural gas and condensate oil:

$$\rho_{\mathrm{g,wf}} Q_{\mathrm{g}} = \rho_{\mathrm{o,sc}} q_{\mathrm{o,sc}} + \rho_{\mathrm{g,sc}} q_{\mathrm{g,sc}} \tag{11}$$

Substituting the wellhead condensate oil production formula into the above equation, the relationship of gas flow rate between bottom-hole and wellhead is obtained as

$$Q_{\mathrm{g}} = E_1 \times q_{\mathrm{g,sc}}, \tag{12}$$

$$E_2 = \frac{\left\{\rho_{\mathrm{o,sc}} V_{\mathrm{roCCE}}(p_{\mathrm{sc}}) + \rho_{\mathrm{g,sc}}\left[1 - V_{\mathrm{roCCE}}(p_{\mathrm{sc}})\right]\right\}\left[1 - V_{\mathrm{roCCE}}\left(p_{\mathrm{wf}}\right)\right]}{\left\{\rho_{\mathrm{o,wf}} V_{\mathrm{roCCE}}\left(p_{\mathrm{wf}}\right) + \rho_{\mathrm{g,wf}}\left[1 - V_{\mathrm{roCCE}}\left(p_{\mathrm{wf}}\right)\right]\right\}\left[1 - V_{\mathrm{roCCE}}(p_{\mathrm{sc}})\right]}, \tag{18}$$

where, E_1 is the conversion factor between bottom-hole flow rate and wellhead flow rate before retrograde condensate, which is expressed as

$$E_1 = \frac{\rho_{\mathrm{o,sc}} V_{\mathrm{roCCE}}(p_{\mathrm{sc}}) + \rho_{\mathrm{g,sc}}[1 - V_{\mathrm{roCCE}}(p_{\mathrm{sc}})]}{\rho_{\mathrm{g,wf}}[1 - V_{\mathrm{roCCE}}(p_{\mathrm{sc}})]} \tag{13}$$

4.2. Relationship of flow rate between bottom-hole and well-head after retrograde condensation

When the retrograde condensation occurs and the gas condensate well produces steadily, the wellhead fluid composition is the same as that of underground and original fluid, no matter whether the condensate oil flows or not. Steady-state means that the reservoir pressure distribution and condensate oil saturation distribution do not change with time. Because the outflow and the precipitation of the condensate oil reach dynamic equilibrium at the same location, the condensate oil saturation does not change, and the composition of the outflow fluid is equal to that of original fluid.

According to CCE, the condensate oil volume fraction of the mixture under the wellhead condition is expressed as Eq. (9), and the wellhead condensate oil production is displayed as Eq. (10).

As the bottom-hole fluid composition is equal to that of the wellhead condensate fluid mixture under steady state, which accords with the principle of constant component expansion (CCE), the condensate oil volume fraction of the mixture under the bottom-hole condition is expressed as

$$V_{\mathrm{roCCE}}\left(p_{\mathrm{wf}}\right) = \frac{V_{\mathrm{o}}}{V_{\mathrm{g}} + V_{\mathrm{o}}} = \frac{Q_{\mathrm{o}}}{Q_{\mathrm{g}} + Q_{\mathrm{o}}} \tag{14}$$

Transforming the above formula, the bottom-hole condensate oil production can be obtained as

$$Q_{\mathrm{o}} = \frac{Q_{\mathrm{g}} V_{\mathrm{roCCE}}\left(p_{\mathrm{wf}}\right)}{1 - V_{\mathrm{roCCE}}\left(p_{\mathrm{wf}}\right)} \tag{15}$$

Although the condensate oil does not flow in the vicinity of the reservoir when the condensate saturation is less than the critical flowing condensate saturation, the condensate oil still flows in the bottom-hole wellbore. By using the law of mass conservation, the equation below is obtained

$$\rho_{\mathrm{o,wf}} Q_{\mathrm{o}} + \rho_{\mathrm{g,wf}} Q_{\mathrm{g}} = \rho_{\mathrm{o,sc}} q_{\mathrm{o,sc}} + \rho_{\mathrm{g,sc}} q_{\mathrm{g,sc}} \tag{16}$$

Substituting the condensate oil production formula of wellhead and bottom-hole into Eq. (16), the relationship of gas production between the wellhead and the bottom-hole can be given as

$$Q_{\mathrm{g}} = E_2 \times q_{\mathrm{g,sc}}, \tag{17}$$

where E_2 is the conversion factor between the bottom-hole production and the wellhead production after retrograde condensation.

5. Deliverability equations of gas condensate well considering the fluid phase behavior in both reservoir and wellbore

5.1. Deliverability equation of gas condensate well before retrograde condensation

In case that condensate gas well is produced at a low gas production rate, the BHFP is higher than the dew point pressure, and the steady state is achieved for any well configuration (such as vertical wells, fractured vertical wells, or horizontal wells), the deliverability equation before retrograde condensation can be combined into the same formula

$$Q_g = C\frac{k_{rg}(S_{wi})}{\rho_{g,wf}}\int_{p_{wf}}^{p_e}\left(\frac{\rho_g}{\mu_g}\right)dp \tag{19}$$

$$C = \frac{2\pi a_1 kh}{\ln\left(r_e/r_w\right) - 0.75 + S} \tag{20}$$

where a_1 is the unit conversion factor; for SI unit system, $a_1 = 1$. Q_g is the bottom-hole gas flow rate. C includes basic reservoir properties, such as the reservoir permeability k, thickness h, gas drainage radius r_e, wellbore radius r_w, and other parameters. Relative permeability k_{rg} and k_{ro} are related with the absolute permeability, rather than the permeability under the irreducible water saturation condition. S is skin factor, which is a combination of factors including some non-ideal flow effects, such as damage, stimulation, drainage geometry, and partial perforation.

Substituting Eqs. (12) and (13) into Eq. (19) gives the gas deliverability equation of gas condensate well before retrograde condensation in the reservoir, which is shown below

$$q_{g,sc} = C \times \frac{1 - V_{roCCE}(p_{sc})}{\rho_{o,sc}V_{roCCE}(p_{sc}) + \rho_{g,sc}[1 - V_{roCCE}(p_{sc})]}k_{rg}(S_{wi}) \times \int_{p_{wf}}^{p_e}\left(\frac{\rho_g}{\mu_g}\right)dp, \tag{21}$$

where C is expressed as Eq. (20).

5.2. Deliverability equation of gas condensate well after retrograde condensation

In case that the gas production of gas condensate well is large, the BHFP is less than the dew point pressure of the original fluid and condensate oil appears in the bottom hole, the deliverability equation of condensate gas well can be written as

$$Q_g = \frac{C\beta_s}{\rho_{g,wf}}\left(\psi_e - \psi_{wf}\right) \tag{22}$$

where β_s is the proportion of the bottom-hole gas phase mass in the total mass of condensate oil and gas system, which is

$$\beta_s = \frac{\rho_{g,wf}Q_g}{\rho_{g,wf}Q_g + \rho_{o,wf}Q_o} \tag{23}$$

Substituting Eq. (15) into Eq. (23) gives

$$\beta_s = \frac{\rho_{g,wf}}{\rho_{g,wf} + \rho_{o,wf}\frac{V_{roCCE}(p_{wf})}{1-V_{roCCE}(p_{wf})}} \tag{24}$$

After retrograde condensation, both condensate oil and gas flow into the wellbore, so the conversion factor between the bottom-hole production and the wellhead production E_2 should be used. Substituting Eqs. (17), (18) and (24) into Eq. (22) gives the gas deliverability equation of gas condensate well after retrograde condensation, which is shown below

$$q_{g,sc} = C \times \frac{1 - V_{roCCE}(p_{sc})}{\rho_{o,sc}V_{roCCE}(p_{sc}) + \rho_{g,sc}[1 - V_{roCCE}(p_{sc})]} \times \left(\psi_e - \psi_{wf}\right) \tag{25}$$

When the BHFP is less than the dew point pressure of the original fluid but higher than p^*_{up}, the condensate oil saturation is less than the critical flowing condensate saturation, and the steady state is achieved, there exists retrograde condensate blockage near the wellbore and only single-phase gas flows in the reservoir; pseudo-pressure difference for two zone model should be used, which is shown as Eq. (4).

In case that the BHFP is less than p^*_{up} but higher than p^*_{down}, the condensate oil saturation is larger than the critical flowing condensate saturation and the steady state is achieved, both condensate oil and gas flow in the reservoir and the wellbore, pseudo-pressure difference for three zone model should be used, which is shown as Eq. (6).

With proration of condensate gas well increasing further, when the BHFP decreases to p^*_{down}, the condensate oil in the near-wellbore region re-evaporates, which reduces the saturation of the near-wellbore condensate oil and makes the condensate oil immobile. From the region far away from the wellbore to the near wellbore region, the condensate oil changes from stagnant to mobile, then to stagnant again, so pseudo-pressure difference for four zone model should be used, which is shown as Eq. (8). It usually happens in gas condensate well with high temperature.

5.3. Deliverability equation of gas condensate well for the whole production process

From comparing deliverability equations of gas condensate well before and after retrograde condensation, it can be clearly seen that deliverability equations during the whole production life are in the same form, which is expressed as

$$q_{g,sc} = C \times E \times \left(\psi_e - \psi_{wf}\right) \tag{26}$$

where E is expressed as

$$E = \frac{1 - V_{roCCE}(p_{sc})}{\rho_{o,sc}V_{roCCE}(p_{sc}) + \rho_{g,sc}[1 - V_{roCCE}(p_{sc})]} \tag{27}$$

In view of the ease used, the condensate oil volume fraction of the mixture under wellhead condition $V_{roCCE}(p_{sc})$ can be transformed as

$$V_{roCCE}(p_{sc}) = \frac{1}{1 + GOR} \tag{28}$$

where GOR is gas oil ratio at the wellhead condition, which can be obtained from PVT experiments. Thus, E will be

$$E = \frac{GOR}{\rho_{o,sc} + \rho_{g,sc}GOR} \tag{29}$$

In Eq. (26), pseudo-pressure difference $(\psi_e - \psi_{wf})$ is different at different stages; the corresponding pseudo-pressure functions are shown as Eqs. (2), (4), (6) and (8); the gas density ρ_g can be expressed as

$$\rho_g = \frac{0.02896\gamma_g p}{ZRT} \tag{30}$$

where the variable is in SI unit system; $R = 8.471$ Pa m^3/(mol K).

After the gas production is determined, the condensate

deliverability equation of gas condensate well can be obtained by dividing gas production by *GOR*.

6. Calculation procedures of gas condensate deliverability

In order to calculate gas and condensate IPR curves by applying the proposed model, the following steps are recommended.

(1) Collect reservoir properties, including absolute permeability, formation thickness, reservoir area, wellbore radius, skin factor, initial reservoir pressure, and reservoir temperature. In these reservoir properties, absolute permeability can be acquired from rock test, well logging, or well testing; formation thickness is from well logging; reservoir area is from geological research; the wellbore radius is from well drilling and completion; the skin factor, initial reservoir pressure and reservoir temperature are from well testing.
(2) Collect fluid properties, including gas specific gravity, Z factor of gas at surface condition, oil density at surface condition, *GOR* at surface condition, and some relationships of Z factor of gas, gas viscosity, oil density, and oil viscosity versus pressure at the reservoir temperature, which are mostly from experiments and polynomial fitting.
(3) Collect upper dew point pressure, the lower dew point pressure, the maximum liquid saturation point pressure $p_{max,So}$, and relationship of condensate oil saturation versus pressure, which are from constant compositional expansion (CCE) experiment and data fitting.
(4) Collect the critical flowing condensate saturation, residual gas saturation, relative permeability curves for gas and condensate oil, the irreducible water saturation, and relative permeability curves for condensate oil and water.
(5) Calculate relationships of gas and condensate oil relative permeabilities versus pressure.
(6) Calculate the upper mobile condensate point pressure p^*_{up} and the lower mobile condensate point pressure p^*_{down}.
(7) Calculate the pseudo-pressure difference for different condensate distribution and flow models of gas condensate reservoir. During calculation, the relationships of gas density, gas viscosity, gas relative permeability, condensate oil density, condensate oil viscosity, and condensate oil relative permeability versus pressure, the upper dew point pressure, the lower dew point pressure, the upper mobile condensate point pressure p^*_{up} and the lower mobile condensate point pressure p^*_{down} are needed.
(8) Calculate the coefficients C and E based on reservoir and fluid parameters.
(9) Calculate the gas production rate of gas condensate well for different BHFPs based on C, E, and the pseudo-pressure

Table 1
Reservoir and fluid properties for two synthetic numerical simulation cases.

Parameters	Simulation Case I	Simulation Case II
p_e (Pa)	51.71×10^6	54×10^6
$p_{d,up}$ (Pa)	49.75×10^6	52.496×10^6
T (K)	412.56	408.85
k (m^2)	19.4×10^{-15}	20×10^{-15}
$k_{rg}(S_{wi})$ (fraction)	0.7828	0.8284
h (m)	3	3
$\rho_{g(sc)}$ (kg/m^3)	0.9343	0.7461
r_e (m)	2380	2380
r_w (m)	0.1	0.1
S (dimensionless)	0	0
$\gamma_{g(sc)}$ (fraction)	0.636	0.63
$\rho_{o(sc)}$ (kg/m^3)	785.4	798.2
S_{wi} (fraction)	0.4108	0.34

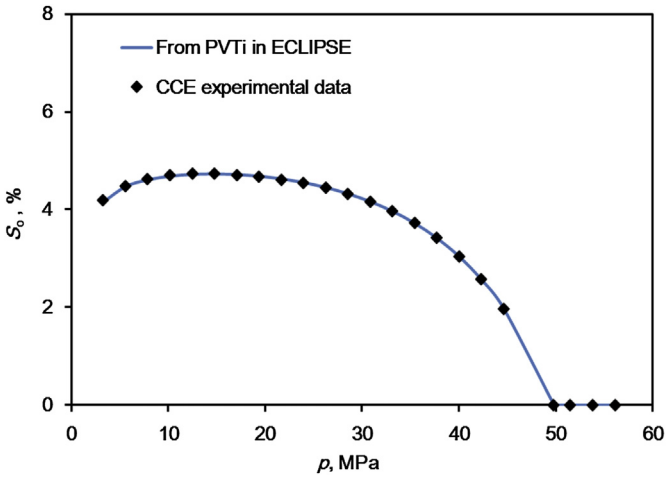

Fig. 2. Plot of condensate oil saturation versus pressure for Simulation Case I.

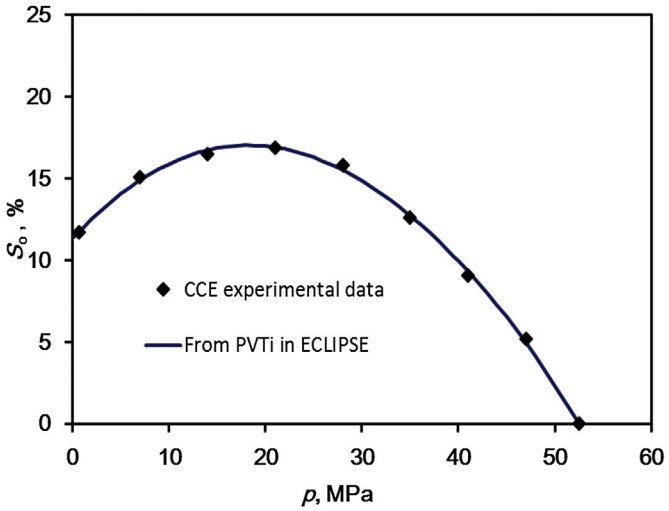

Fig. 3. Plot of condensate oil saturation versus pressure for Simulation Case II.

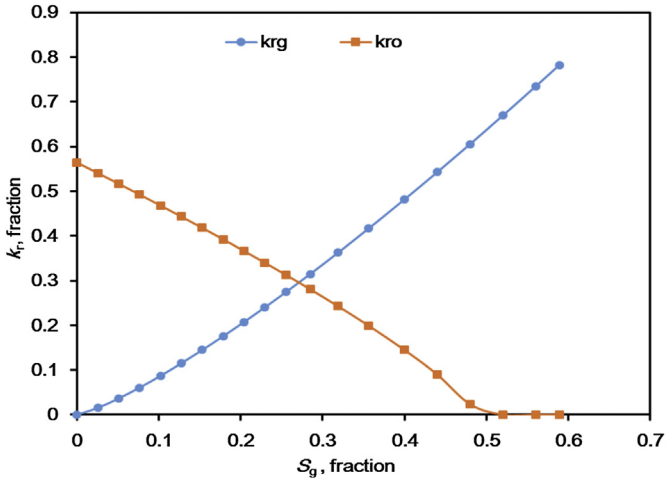

Fig. 4. Relative permeability curves from Yakela gas condensate reservoir for Simulation Case I.

difference by using Eq. (26), and draw the gas IPR curve for the gas condensate well.

(10) Calculate the condensate production rate by using the corresponding gas production rate and *GOR*.

In the calculation process of gas condensate deliverability using the above ten steps, almost all collected parameters are necessary except that gas drainage radius and condensate oil relative permeability are adjusted parameters.

7. Validation by synthetic numerical simulation and field cases

7.1. Validation by synthetic numerical simulation cases

Two synthetic numerical simulations are conducted to validate the proposed deliverability equation for gas condensate wells. Simulation Case I has low condensate content, and Simulation Case II has high condensate content. The reservoir and fluid properties for these two synthetic numerical simulation cases are listed in Table 1. Fluid composition, PVT experiments, and relative permeability curves for Simulation Case I and Simulation Case II are from Yakela gas condensate reservoir and Yaha gas condensate reservoir, respectively. The relationship of condensate oil saturation versus pressure from the CCE experiment and PVT matched by PVTi in ECLIPSE for Simulation Case I and Simulation Case II are shown in Figs. 2 and 3, respectively; it can be seen that the condensate saturations from PVTi match the experimental data very well. The relative permeability data from laboratory for Simulation Case I and Simulation Case II are shown in Figs. 4 and 5, respectively.

By applying reservoir simulator ECLIPSE, the gas condensate reservoirs with parameters in Table 1, Figs. 2–5 were established, as shown in Fig. 6. The grid number of the gas condensate reservoir in X, Y, and Z directions are 101, 101, and 2 respectively; the well is located in the middle of the reservoir with X–Y coordinate of (51, 51), and the grid size in X direction is 40 m except that for 13 grids near the wellbore it is 3 m for the purpose of accuracy and that for 20 grids far away from the wellbore it is 100 m for the purpose of rapid calculation. The grid size in Y direction is set in the same way.

7.1.1. Simulation Case I

For Simulation Case I, BHFPs for different gas flow rates decreased with production time and almost stabilized after 15 days' production, as shown in Fig. 7. From Fig. 8, we can see that the

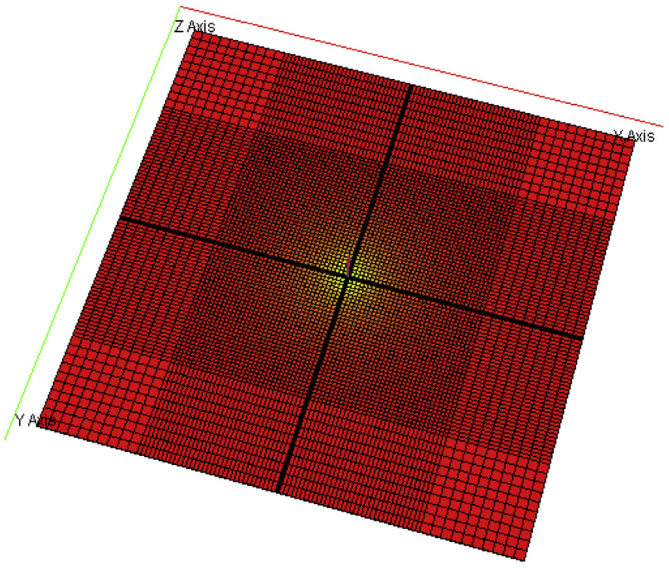

Fig. 6. The geological model for two synthetic simulation cases.

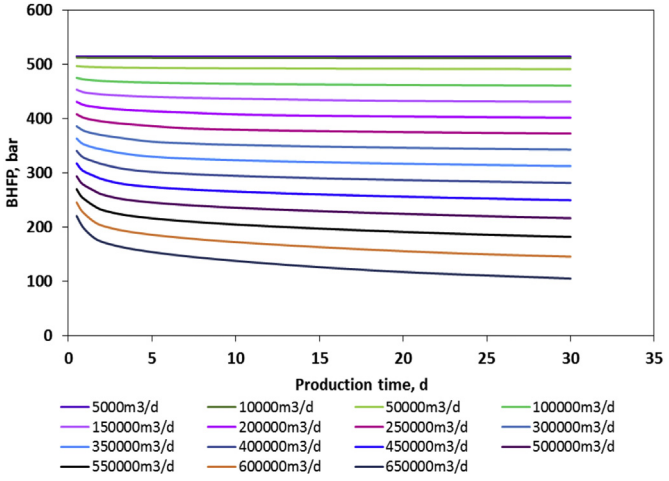

Fig. 7. The plot of BHFPs for different gas flow rates versus production time for Simulation Case I.

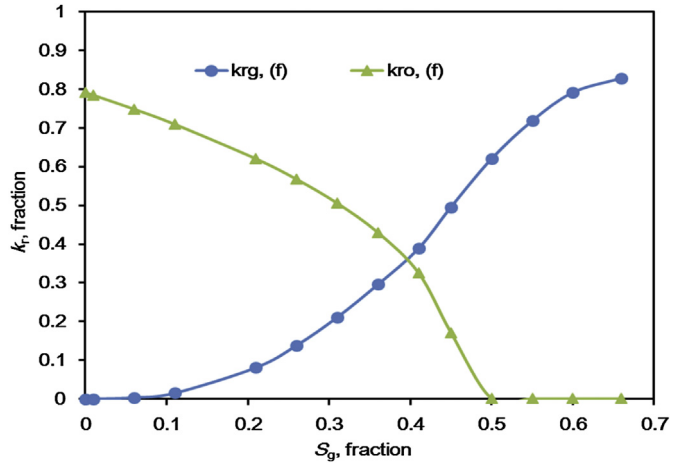

Fig. 5. Relative permeability curves from Yaha gas condensate reservoir for Simulation Case II.

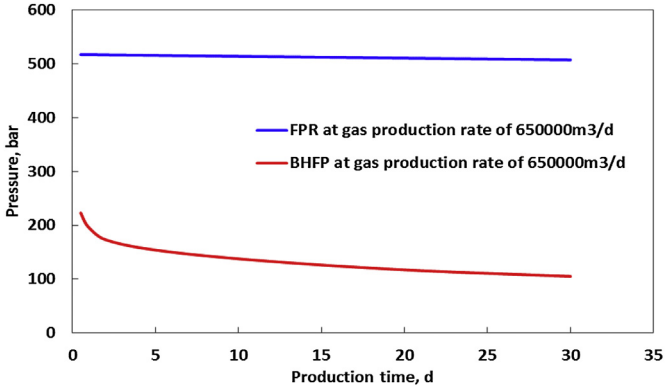

Fig. 8. The plot of BHFP and formation pressure (FPR) versus production time for Simulation Case I with a gas flow rate of 650,000 m^3/d.

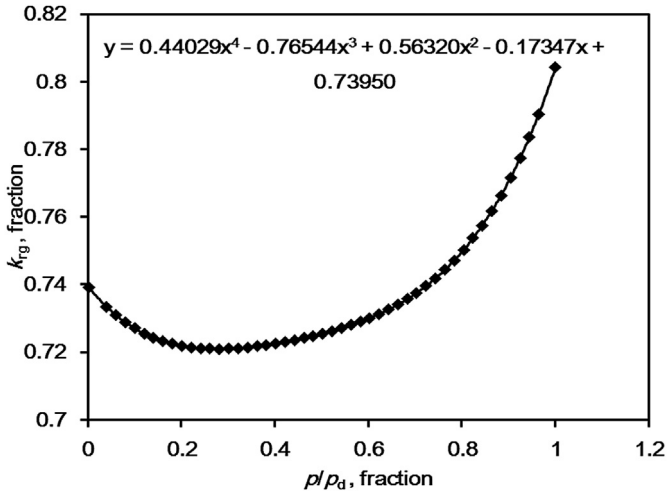

Fig. 9. Relationship between k_{rg} and $p/p_{d,up}$ for Simulation Case I.

formation pressure (FPR) almost does not decrease after 30 days of production, even for the largest gas flow rate of 650,000 m^3/d.

On the other hand, the productivity of the gas condensate well is calculated by the proposed equations. The relationship of k_{rg} versus $p/p_{d,up}$ can be easily obtained by combining the relationship of condensate saturation versus pressure (Fig. 2) and the relationship of gas relative permeability versus the condensate saturation (Fig. 4). Based on the correlation proposed by Shi et al. (2013), when the pressure is below the upper dew point pressure, the modified correlation of the gas relative permeability versus the ratio of the pressure and the upper dew point pressure is expressed as

$$k_{rg} = c_5\left(\frac{p}{p_d}\right)^5 + c_4\left(\frac{p}{p_d}\right)^4 + c_3\left(\frac{p}{p_d}\right)^3 + c_2\left(\frac{p}{p_d}\right)^2 + c_1\left(\frac{p}{p_d}\right) + c_0,\ p \le p_d \tag{31}$$

The relationship of k_{rg} versus $p/p_{d,up}$ in Simulation Case I is presented in Fig. 9.

From Fig. 9 and Eq. (31), coefficients in Eq. (31) can be obtained: $c_5 = 0$, $c_4 = 0.44029$, $c_3 = -0.76544$, $c_2 = 0.5632$, $c_1 = -1.17347$, and $c_0 = 0.7395$.

The deliverability equation of gas condensate well considering the fluid phase behavior in both the reservoir and the wellbore for Simulation Case I can be obtained from Eq. (26).

As shown in Fig. 2, the highest condensate saturation precipitated in the formation is 4.73%. Since the initial irreducible water saturation is 41.08%, the maximum gas saturation is 58.92%. From Fig. 3, it can be seen that the gas saturation is 52% when condensate begins to flow; hence the critical flowing condensate saturation is about 7%, which is larger than condensate saturation precipitated in the formation; condensate cannot flow in porous media after precipitation. Thus, the calculation of the pseudo-pressure difference in the deliverability equation of gas condensate well considering the fluid phase behavior in both the reservoir and wellbore can be divided into two stages. When the retrograde condensation does not occur in the reservoir, particularly when the BHFP is higher than the dew point pressure, the pseudo-pressure difference can be calculated by Eq. (2). When the retrograde condensation occurs but condensate does not flow, specifically when the BHFP is less than the dew point pressure, the pseudo-pressure difference can be calculated by Eq. (4).

In order to verify the effectiveness of the proposed deliverability equations of gas condensate well, the conventional gas deliverability equation of gas condensate well and the conventional gas deliverability equation of dry gas well are introduced to conduct a comparison. The conventional gas deliverability equation of gas condensate well considering only fluid phase behavior in the reservoir and the conventional gas deliverability equation of dry gas well without considering fluid phase behavior, in which the volume factor B_g at bottom-hole condition are both applied, can be written in the same form

$$q_{g,sc} = \frac{C}{\rho_{g,wf} B_g}\left(\psi_e - \psi_{wf}\right) \tag{32}$$

where $(\psi_e - \psi_{wf})$ for dry gas well without considering fluid phase behavior is Eq. (2), while $(\psi_e - \psi_{wf})$ for gas condensate well considering only fluid phase behavior in the reservoir is expressed as

$$\psi_e - \psi_{wf} = k_{rg}(S_{wi}) \int_{p_{d,up}}^{p_e} \left(\frac{\rho_g}{\mu_g}\right) dp + \int_{p_{wf}}^{p_{d,up}} \left(\rho_g \frac{k_{rg}}{\mu_g}\right) dp \tag{33}$$

The comparison of gas IPR curves of the gas condensate well by using numerical simulation and three different deliverability equations for Simulation Case I is shown in Fig. 10.

From Fig. 10, it can be seen that the difference between gas

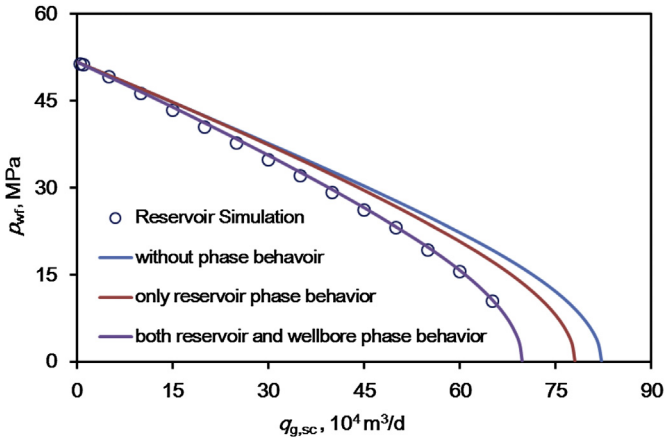

Fig. 10. Comparison of gas IPR curves of gas condensate well by using numerical simulation and three different deliverability equations for Simulation Case I.

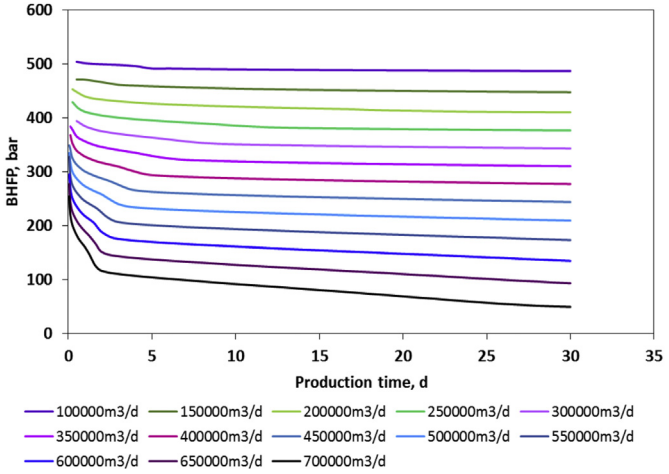

Fig. 11. The plot of BHFPs for different gas flow rates versus producing time for Simulation Case II.

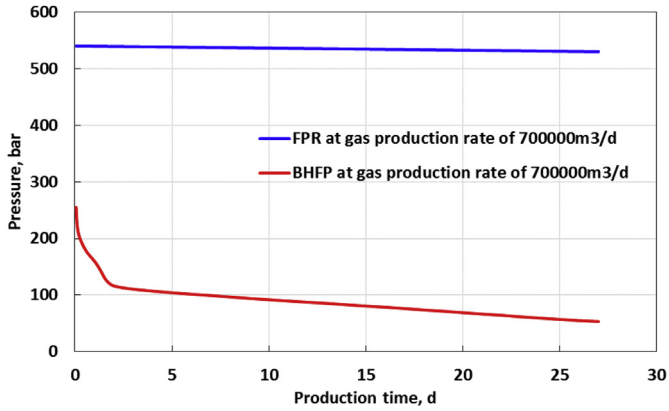

Fig. 12. The plot of BHFP and formation pressure (FPR) versus producing time for Simulation Case II with gas flow rate of 700,000 m^3/d.

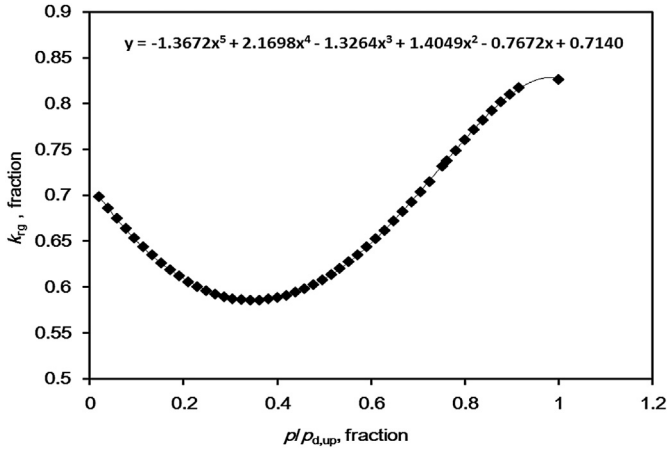

Fig. 13. Relationship between k_{rg} and $p/p_{d,up}$ for Simulation Case II.

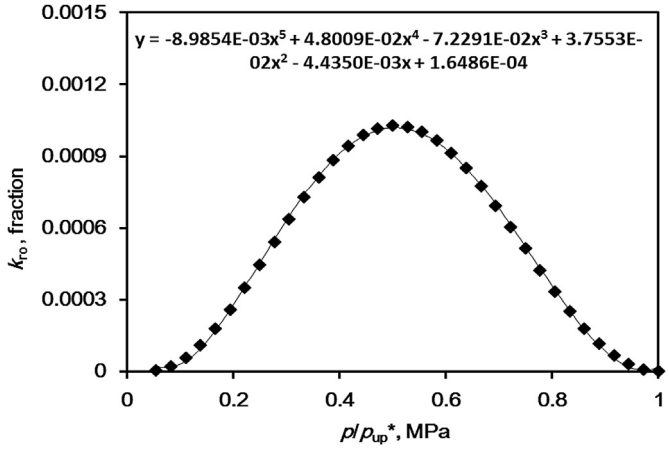

Fig. 14. Relationship between k_{ro} and p/p^*_{up} for Simulation Case II.

production rates calculated by three different deliverability equations is gradually increasing with decreasing BHFP, especially in the late stage of condensate gas production. The AOF of natural gas calculated by the deliverability equation without considering fluid phase behavior in the reservoir and wellbore, by deliverability equation considering only fluid phase behavior in the reservoir, and by deliverability equation considering the fluid phase behavior in both the reservoir and wellbore, are about 82×10^4 m^3/d, 78×10^4 m^3/d, and 69×10^4 m^3/d, respectively. Although the difference in the AOF of natural gas calculated by these three deliverability equations is not very significant owing to the low condensate content in this simulation case, a good agreement was obtained between simulated natural gas production and those forecasted by the deliverability equation considering fluid phase behavior in both the reservoir and wellbore.

7.1.2. Simulation Case II

In Simulation Case II, BHFPs for different gas flow rates decrease with production time and almost stabilize after 15 days' production, as shown in Fig. 11. Fig. 12 indicates that the formation pressure (FPR) almost remains constant after 30 days of production with the largest gas flow rate of 700,000 m^3/d.

On the other hand, the deliverability of the gas condensate well was calculated by the proposed equations. The relationships of k_{rg} versus $p/p_{d,up}$ and k_{ro} versus p/p^*_{up}, as shown in Figs. 13 and 14, can be easily obtained by combining the relationship of condensate saturation versus pressure (Fig. 3) and the relationship of relative permeability versus the condensate saturation (Fig. 5).

The deliverability equation of gas condensate well considering the fluid phase behavior in both the reservoir and the wellbore for Simulation Case II can be obtained by Eq. (26).

As shown in Fig. 3, the highest condensate saturation precipitated in the formation is about 17%. Since the initial irreducible water saturation is 34%, the maximum gas saturation is 66%. From Fig. 5, it can be seen that the gas saturation is about 54% when condensate begins to flow; so the critical flowing condensate saturation is about 12%, and the corresponding p^*_{up} and p^*_{down} are 36 MPa and 2 MPa, respectively.

Thus, the calculation of pseudo-pressure difference in the deliverability considering the fluid phase behavior in both the reservoir and wellbore can be divided into four stages, namely single gas flow ($p_{wf} > p_{d,up}$), gas flow with stagnant condensate ($p^*_{up} < p_{wf} < p_{d,up}$), gas and condensate two phase flow ($p^*_{down} < p_{wf} < p^*_{up}$), and gas flow with stagnant condensate changed from mobile condensate ($p_{wf} < p^*_{down}$), and the corresponding pseudo-pressure difference can be calculated by Eqs. (2), (4), (6) and (8).

The comparison of gas IPR curves of the gas condensate well by using numerical simulation and three different deliverability equations for Simulation Case II is shown in Fig. 15.

As shown in Fig. 15, a good agreement was obtained between

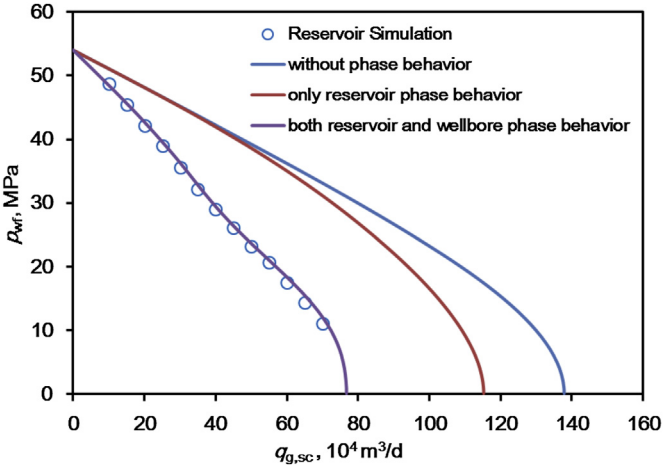

Fig. 15. Comparison of gas IPR curves of gas condensate well by using numerical simulation and three different deliverability equations for Simulation Case II.

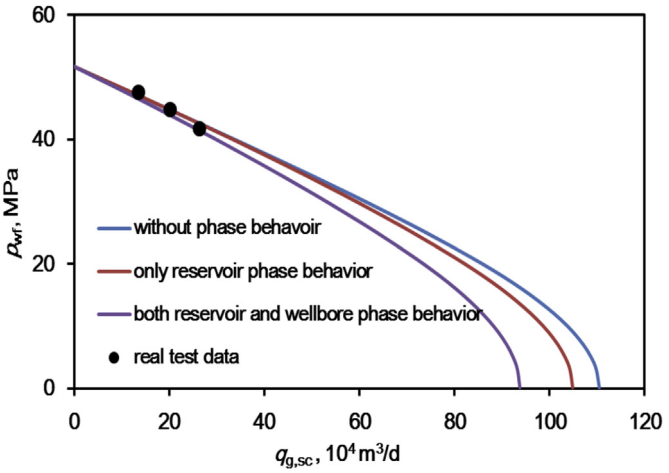

Fig. 16. Comparison of gas IPR curves of gas condensate well by using three different deliverability equations and the field data for Field Case I.

simulated natural gas production and those forecasted by the deliverability equation considering fluid phase behavior in both the reservoir and wellbore. However, the gas IPR curves forecasted by the deliverability equations without considering phase behavior in reservoir or wellbore greatly deviate from the simulated data. For this simulation case, the AOF of natural gas calculated by the deliverability equation without considering fluid phase behavior in the reservoir and wellbore, by deliverability equation considering only fluid phase behavior in the reservoir, and by deliverability equation considering fluid phase behavior in both the reservoir and wellbore, are about 137 $\times$ 10^4 m^3/d, 115 $\times$ 10^4 m^3/d, and 77 $\times$ 10^4 m^3/d, respectively.

From these two synthetic simulation cases, we can conclude that the gas deliverability equation considering the fluid phase behavior in both the reservoir and the wellbore is more accurate to forecast gas and condensate oil production. If using deliverability equations without considering fluid phase behavior and considering only phase behavior in the reservoir, the gas production from this gas condensate well will be overestimated, especially at the lower BHFP stage.

7.2. Validation by field cases

7.2.1. Field Case I

The difference between deliverability equations with and without considering fluid phase behavior in the reservoir and wellbore is also illustrated by field case studies. In Field Case I, a well in Yakela gas condensate reservoir is analyzed. Except for h = 2.93 m, r_e = 86.94 m, and S = 0.76, which are from transient pressure interpretation, other reservoir and fluid properties for this field case are same as those for Simulation Case I, as listed in Table 1. In addition, the relationship of condensate oil saturation versus pressure from the CCE experiment and the relative permeability data from laboratory for this real case are also same as those for Simulation Case I, as shown in Figs. 2 and 4.

Comparison of gas IPR curves of the gas condensate well by using three different deliverability equations and field data is shown in Fig. 16.

The AOF of natural gas calculated by the deliverability equation without considering fluid phase behavior in the reservoir and wellbore, by deliverability equation considering only fluid phase behavior in the reservoir, and by deliverability equation considering the fluid phase behavior in both the reservoir and wellbore, are about 111 $\times$ 10^4 m^3/d, 105 $\times$ 10^4 m^3/d, and 94 $\times$ 10^4 m^3/d, respectively. Owing to low condensate saturation in the reservoir, at high BHFP stage gas production rates by these three deliverability equations are all close to the field data, but the gas production rates forecasted by deliverability equation considering the fluid phase behavior in both the reservoir and wellbore are much closer to the field data.

Table 2
Reservoir and fluid properties for Real Case II.

Parameters	Values
p_e (Pa)	51.529 $\times$ 10^6
$p_{d,up}$ (Pa)	49.37 $\times$ 10^6
T (K)	411
kh (m^2 m)	38.24 $\times$ 10^{-15}
$k_{rg}(S_{wi})$ (fraction)	0.8284
p_{up}^* (Pa)	44 $\times$ 10^6
$\rho_{g(sc)}$ (kg/m^3)	0.7461
r_e (m)	170
r_w (m)	0.089
S (dimensionless)	2.75
$\gamma_{g(sc)}$ (fraction)	0.63
$\rho_{o(sc)}$ (kg/m^3)	798.2
S_{wi} (fraction)	0.34

7.2.2. Field Case II

In Field Case II, another gas well in Yaha gas condensate reservoir with high condensate oil content is analyzed. The reservoir and fluid properties for this case are presented in Table 2; the formation coefficient kh is from transient pressure interpretation; condensate oil saturation versus pressure from the CCE experiment is shown in Fig. 17, and the relative permeability data from laboratory for this field case is shown in Fig. 18.

As shown in Table 2, the irreducible water saturation is 34%. From Fig. 18, it can be seen that the gas saturation is 45% when condensate begins to flow; hence the critical condensate saturation is 21%. From Fig. 17, we can get that p_{up}^* is 44 MPa; so the calculation of pseudo-pressure difference in the deliverability considering the fluid phase behavior in both the reservoir and wellbore can be divided into three stages, namely single gas flow ($p_{wf} > p_{d,up}$), gas flow with stagnant condensate ($p_{up}^* < p_{wf} < p_{d,up}$), and gas and condensate two phase flow ($p_{wf} < p_{up}^*$); the corresponding pseudo-pressure difference can be calculated by Eqs. (2), (4) and (6).

The relationships of k_{rg} vs $p/p_{d,up}$ and k_{ro} vs p/p_{up}^* for this field case are presented in Figs. 19 and 20, respectively.

Comparison of gas IPR curves of the gas condensate well by using Eqs. (2), (32) and (33), the proposed deliverability equation (Eq. (26)), and the field data is shown in Fig. 21.

Owing to the high condensate saturation in the reservoir, the difference among AOFs of natural gas calculated by three different equations is significant. The AOF of natural gas calculated by the deliverability equation without considering fluid phase behavior in the reservoir and wellbore, by deliverability equation considering only fluid phase behavior in the reservoir, and by deliverability equation considering fluid phase behavior in both the reservoir and wellbore, are about 87 $\times$ 10^4 m^3/d, 50 $\times$ 10^4 m^3/d, and 36 $\times$ 10^4 m^3/d, respectively. The gas production rates predicted by the deliverability equation considering the fluid phase behavior in both the reservoir and wellbore are in good agreement with the field data.

The results of synthetic numerical simulation cases and field case studies verify that the proposed deliverability equation of condensate gas well in this work is more appropriate to forecast the production of condensate gas well.

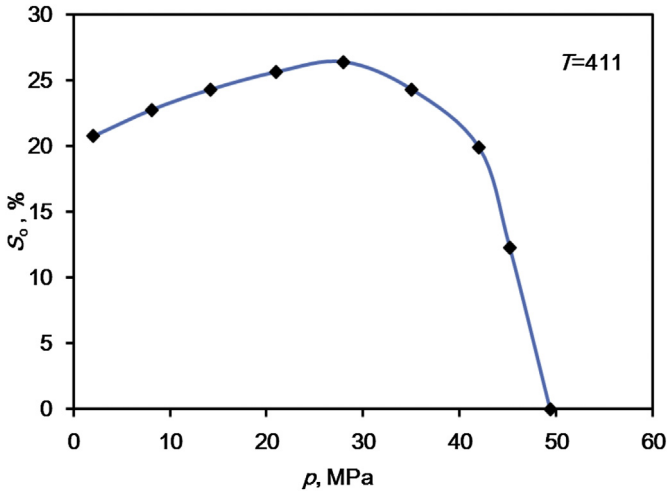

Fig. 17. Plot of condensate oil saturation versus pressure from the CCE experiment for Field Case II.

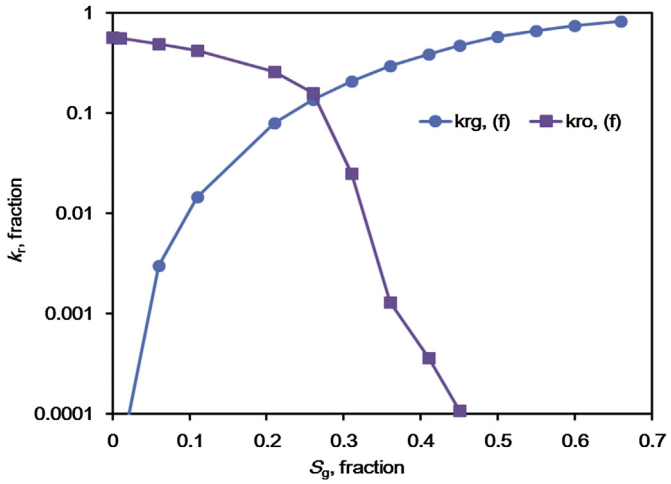

Fig. 18. Relative permeability data from laboratory for Field Case II.

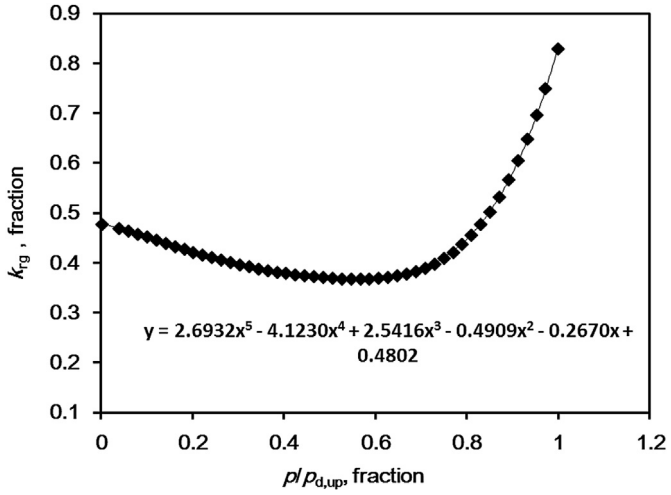

Fig. 19. Relationship between k_{rg} and $p/p_{d,up}$ for Field Case II.

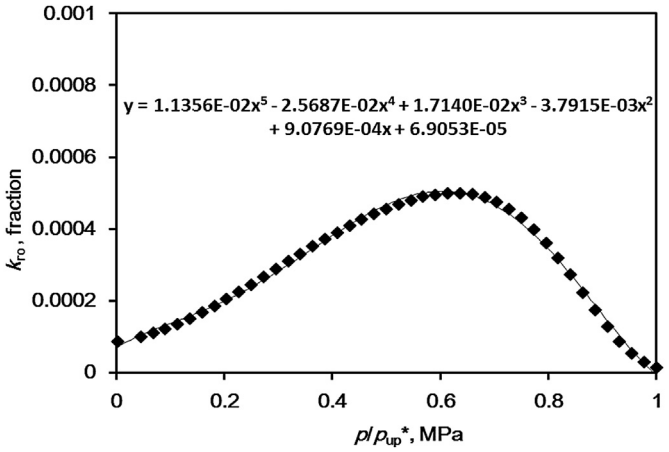

Fig. 20. Relationship between k_{ro} and p/p^*_{up} for Real Case II.

8. Conclusions

(1) There are complex fluid phase behaviors in the reservoir and wellbore for the condensate oil and gas system. The conventional deliverability equation of gas condensate well merely considers fluid phase behavior in the reservoir, but ignores fluid phase behavior in the wellbore. In this paper, a new deliverability equation of gas condensate well considering the fluid phase behavior in both the reservoir and the wellbore is proposed, which is more in line with the simulated and the actual dynamic performance of gas condensate wells.

(2) Currently, the wellhead productions of gas and condensate oil are directly converted from production data in the bottom-hole by using the volume factor. As a matter of fact, volume factor is not expected to exist in the pseudo-pressure function, because wellhead production cannot be directly converted from bottom-hole production by using volume factor for gas condensate well due to the fluid phase behavior in the wellbore. In this work, different pseudo-pressure functions for different regions are obtained according to condensate distribution in the vicinity of gas condensate well. Pseudo-pressure function is determined by values of parameters in each region. The total pseudo-pressure difference in the deliverability equation of gas condensate well is the sum of pseudo-pressure differences in each region.

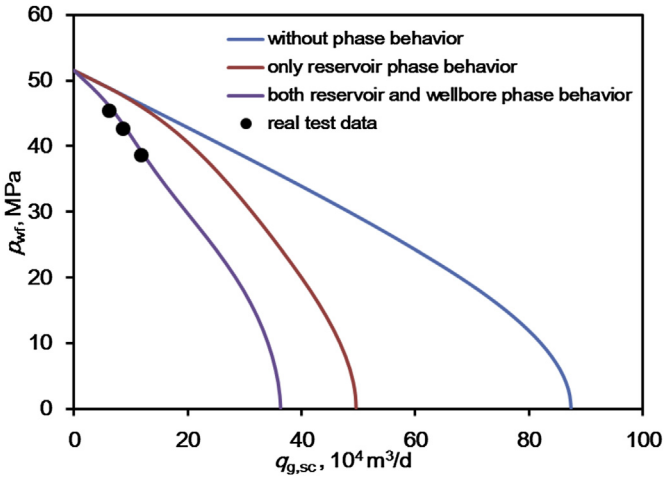

Fig. 21. Comparison between gas IPR curves of the gas condensate well by using different deliverability equations and the field data for Field Case II.

(3) Two synthetic numerical simulation cases and two field case studies validate the proposed deliverability equation of gas condensate well. Results show that the fluid phase behavior in both the reservoir and wellbore should be considered. Considering fluid phase behavior only in the reservoir or neither in the reservoir nor in the wellbore will result in great errors.

Acknowledgment

This study was sponsored by the National Natural Science Foundation of China (U1262113) and Science Foundation of China University of Petroleum, Beijing (YJRC-2013-37). We recognize the support of MOE Key Laboratory of Petroleum Engineering in China University of Petroleum (Beijing) for the permission to publish this article.

Nomenclature

$p_{d,up}$	the upper dew point pressure of gas condensate system, Pa
$p_{d,down}$	the lower dew point pressure of gas condensate system, Pa
p_{wf}	bottom-hole flowing pressure, Pa
BHFP	bottom-hole flowing pressure, Pa
AOF	absolute open flow rate, m^3/d
GOR	gas oil ratio, dimensionless
p_{sc}	pressure at standard state, Pa
p_e	the initial reservoir pressure, Pa
p^*_{up}	the upper mobile condensate point pressure, below which condensate oil begins to flow, Pa
p^*_{down}	the lower mobile condensate point pressure, below which condensate oil stops flowing, Pa
$p_{max,So}$	the maximum liquid saturation point pressure, Pa
S_{wi}	the irreducible water saturation, fraction
k	the absolute permeability, m^2
k_{rg}	gas relative permeability, fraction
$k_{rg}(S_{wi})$	the gas relative permeability at the irreducible water saturation, fraction
ρ_g	gas density at present pressure, kg/m^3
$\rho_{g,sc}$	gas density at standard state, kg/m^3
$\rho_{g,wf}$	gas density at bottom-hole condition, kg/m^3
$\rho_{o,sc}$	condensate density at standard state, kg/m^3
$\rho_{o,wf}$	condensate density at the bottom-hole condition, kg/m^3
μ_g	gas viscosity, Pa·s
$\overline{\mu}$	average gas viscosity, Pa·s
B_g	gas volume factor, dimensionless
$q_{o,sc}$	condensate flow rate at standard state, m^3/s
$q_{g,sc}$	gas flow rate at standard state, m^3/s
Q_g	gas flow rate in the bottom-hole, m^3/s
Q_o	condensate flow rate in the bottom-hole, m^3/s
E_1	conversion factor between bottom-hole flow rate and wellhead production before retrograde condensation, dimensionless
E_2	conversion factor between bottom-hole flow rate and wellhead production after retrograde condensation, dimensionless
$V_{roCCE}(p_{sc})$	the condensate oil volume fraction of the mixture under wellhead condition, dimensionless
$V_{roCCE}(p_{wf})$	the condensate oil volume fraction of the mixture under bottom-hole condition, dimensionless
a_1	the unit conversion factor, for SI unit system, $a_1 = 1$
h	formation net thickness, m
S	Skin factor, dimensionless
r_e	gas drainage radius, m
r_w	wellbore radius, m
$r_{g(sc)}$	gas specific gravity at standard state, dimensionless
T	formation temperature, K
Z	gas deviation factor, dimensionless
$\overline{Z}$	the average gas deviation factor, dimensionless
c_0, c_1, c_2, c_3, c_4, and c_5	coefficients of the gas relative permeability equation, dimensionless
β_s	the proportion of the bottom-hole gas phase mass in the total mass of condensate oil and gas system, dimensionless

References

Ali, J.K., McGauley, P.J., Wilson, C.J., 1997. Experimental Studies and Modeling of Gas Condensate Flow Near the Wellbore. Paper SPE 39053 Presented at the 5th Latin American and Caribbean Petroleum Engineering Conference and Exhibition, Rio De Janairo, Brazil, 30 August-3 September. http://dx.doi.org/10.2118/39053-MS.

Du, Y., Guan, L., Li, D., 2004. Deliverability of Wells in the Gas Condensate Reservoir. Paper SPE 88796 Presented at the 11th Abu Dhabi international Petroleum Exhibition and Conference, Abu Dhabi, United Arab Emirates, 10–13 October. http://dx.doi.org/10.2118/88796-MS.

Fetkovich, M.J., 1973. The Isochronal Testing of Oil Wells. Paper SPE 4529 Presented at the 1973 SPE Annual Technical Conference and Exhibition, Las Vegas, Sept.30-Oct.3. SPE 4529-MS. http://dx.doi.org/10.2118/4529-MS.

Fevang, Φ., Whitson, C.H., 1995. Modeling Gas-condensate Well Deliverability. Paper SPE 30714 Presented at the SPE Annual Technical Conference & Exhibition, Dallas, U.S.A., October 22–25. SPE 30714-MS. http://dx.doi.org/10.2118/30714-MS.

Fussell, D.D., 1972. Single-well Performance Predictions for Gas Condensate Reservoirs. Paper SPE 4072 Presented at SPE-AIME 47th Annual Fall Meeting, San Antonio, TX., Oct. 8–11. SPE 4072-MS. http://dx.doi.org/10.2118/4072-MS.

Gondouin, M., Iffly, R., Husson, J., 1967a. An attempt to predict the time dependence of well deliverability in gas condensate fields. SPE J. 7 (2), 113–124. http://dx.doi.org/10.2118/1478-PA. SPE-1478-PA.

Gondouin, M., Iffly, R., Husson, J., 1967b. An attempt to predict the time dependence of well deliverability in gas condensate fields. SPE J. 7, 113–124. http://dx.doi.org/10.2118/1478-PA. SPE 1478-PA.

He, Z., Sun, L., Li, S., 1996. A new method for deliverability analysis in gas condensate wells. Nat. Gas. Ind. 16, 32–36.

Henderson, G.D., Danesh, A., Tehrani, D.H., Al-Kharusi, B., 2000. The Relative Significance of Positive Coupling and Inertial Effects on Gas Condensate Relative Permeabilities at High Velocity. Paper SPE 62933 Presented at the SPE Annual Technical Conference and Exhibition, Dallas, Texas, 1-4 October. http://dx.doi.org/10.2118/62933-MS.

Houpeurt, A., 1959. On the flow of gases in porous Media. Rev. L' Inst. Fr. Pet. XIV (11), 1468–1684.

Jones, J.R., Raghavan, R., 1985. Interpretation of Flowing Well Response in Gas Condensate Wells. Paper SPE 14204 Presented at the 1985 SPE Annual Technical Conference and Exhibition, Las Vegas, Sept. 22–25. SPE 14204-MS. http://dx.doi.org/10.2118/14204-MS.

Kniazeff, V.J., Naville, S.A., 1965. Two-phase flow of volatile hydrocarbons. SPE J. 37–44.

Li, S., 2008. Natural Gas Engineering. Petroleum Industry Press, Beijing.

Muskat, M., Meres, M.W., 1936. The flow of heterogeneous fluids through porous Media. J. Appl. Phys. 7 (9), 346–363. http://dx.doi.org/10.1063/1.1745403.

O'Dell, H.G., Miller, R.N., 1967. Successfully cycling a low permeability, high-yield gas condensate reservoirs. JPT 41–47.

Rawlins, E.L., Schellhardt, M.A., 1935. Backpressure Data on Natural Gas Wells and Their Application to Production Practices. In: Monograph Series, vol. 7. USBM.

Shi, J., Li, X., Shi, D., Xu, H., Li, B., Zhou, J., 2010. A New Deliverability Testing Method for Gas Condensate Wells. Paper SPE 131443 Presented at the CPS/SPE International Oil & Gas Conference and Exhibition in China, Beijing, China, June 8–10. SPE 131443-MS. http://dx.doi.org/10.2118/131443-MS.

Shi, J., Li, X., Zhou, J., Li, Q., Wu, K., 2013. Deliverability prediction of gas condensate wells based on statistics. Pet. Sci. Technol. 31, 1353–1360.

Whitson, C.H., Fevang, O., Saevareid, A., 1999. Gas Condensate Relative Permeability for Well Calculations. Paper SPE 56476 Presented at the SPE Annual Technical Conference and Exhibition, Dallas, Texas, 3–6 October. http://dx.doi.org/10.2118/56476-MS.

Xie, X., Luo, K., Song, W., 2001. A novel equation for modeling gas condensate well deliverability. Acta.Pet. Sin. 22, 36–42.